Chinese Chemical Letters 37 (2026) 111314

Contents lists available at ScienceDirect

Chinese Chemical Letters

journal homepage: www.elsevier.com/locate/cclet

Daphcalycines A–D, four highly rearranged *Daphniphyllum* alkaloids with cardioprotective activity from *Daphniphyllum calycinum*

Ji-Hui Zhang[a], Hui-Lin Ou[a], Ting Lu[a], Si-Yu Yang[c], Ding Luo[a], Peng Wu[d], Yao-Lan Li[a], Neng-Hua Chen[b,*], Guo-Cai Wang[a,*], Yu-Bo Zhang[a,c,*]

[a] *State Key Laboratory of Bioactive Molecules and Druggability Assessment, and Department of Pharmacology, School of Medicine, Jinan University, Guangzhou 510632, China*
[b] *Department of Pharmacy, The First Affiliated Hospital, Jinan University, Guangzhou 510630, China*
[c] *Guangdong Province Key Laboratory of Pharmacodynamic Constituents of TCM and New Drugs Research, College of Pharmacy, Jinan University, Guangzhou 510632, China*
[d] *Guangdong Provincial Key Laboratory of Translational Cancer Research of Chinese Medicines, Joint International Research Laboratory of Translational Cancer Research of Chinese Medicines, International Institute for Translational Chinese Medicine, School of Pharmaceutical Sciences, Guangzhou University of Chinese Medicine, Guangzhou 510006, China*

ARTICLE INFO

Article history:
Received 5 January 2025
Revised 10 May 2025
Accepted 13 May 2025
Available online 13 May 2025

Keywords:
Daphniphyllum calycinum
Daphniphyllum alkaloid
Biosynthetic pathway
Cardioprotective activity
Keap1-Nrf2/HO-1 pathway

ABSTRACT

Four novel *Daphniphyllum* alkaloids with highly rearranged skeletons involving a 6/5/7/7/5 pentacyclic scaffold (**1**), a 6/5/7/5/6/5/6 heptacyclic scaffold (**2** and **4**), and a 6/5/7/5/6/5 hexacyclic scaffold (**3**), were isolated from *Daphniphyllum calycinum*. Particularly, compound **1** contains a unique 13-oxa-17-aza-pentacyclo[7.6.4.1^{12,15}.0^{4,8}.0^{9,15}] eicosane core. Their structures were elucidated by comprehensive spectroscopic analyses, single-crystal X-ray diffraction, and electronic circular dichroism calculations. Putative biosynthetic pathways for compounds **1–4** were discussed with caldaphnidine C (**5**) as their biosynthetic precursor. Compound **2** markedly enhanced the survival of H9c2 cardiomyocytes under oxygen glucose deprivation and reoxygenation conditions. Mechanistic study revealed that **2** exerted its cardioprotective effects by activating the nuclear factor erythroid 2-related factor 2/heme oxygenase-1 (Nrf2/HO-1) antioxidant pathway, thereby enhancing cellular antioxidant capacity and alleviating oxidative stress induced by hypoxia.

© 2025 Published by Elsevier B.V. on behalf of Chinese Chemical Society and Institute of Materia Medica, Chinese Academy of Medical Sciences.

Acute myocardial infarction (AMI) is a leading cause of death and disability worldwide, especially in developing countries, where its rates are increasing [1]. This is largely due to lifestyle changes, poor diets, and lack of medical resources [1]. Given the concerning rise in AMI incidence, it is crucial to explore drugs specifically aimed at improving the condition of patients with heart disease. Recent research indicates that the natural product formononetin can help protect heart cells by reducing oxidative stress and promoting cell survival, which can lessen damage from ischemia-reperfusion injury [2,3]. Natural products have been proven to be valuable source of bioactive molecules for drug development [4], continued research in this area could provide more therapeutic options for patients suffering from cardiovascular issues.

Daphniphyllum alkaloids (DAs) are a diverse group of natural products from the *Daphniphyllum* genus, characterized by unique azapolycyclic structures with multiple continuous stereogenic centers [5]. These alkaloids exhibit a variety of scaffold types, with this diversity arising from their distinctive biosynthesis, which involves the repeated fission of C–C and/or C–N bonds, followed by rearrangements, decarboxylation, and other reactions [5]. Approximately 360 natural DAs have been reported thus far, some of which exhibit significant biological effects, such as cytotoxic and anti-human immunodeficiency virus (HIV) activities [5–9]. Challenging and caged polycyclic architectures and the promising biological profiles make DAs intriguing targets for natural products and synthetic chemistry [10–16].

Our group has a longstanding interest in exploring medicinal plants to identify natural products with bioactive properties [7,30–32]. The plants of *D. calycinum* have a long history of use in traditional Chinese medicine for treating fever, asthma, inflammation, and influenza [7,9]. Given this medicinal significance and inspired by previous studies revealing the significant structural diversity of DAs in *D. calycinum* [7,17–18], we set out to investigate this species and discovered four novel alkaloids (daphcalycines A–D; Fig. 1),

* Corresponding authors.
E-mail addresses: chennengflo@163.com (N.-H. Chen), twangguocai@jnu.edu.cn (G.-C. Wang), ybzhang99@126.com (Y.-B. Zhang).

https://doi.org/10.1016/j.cclet.2025.111314
1001-8417/© 2025 Published by Elsevier B.V. on behalf of Chinese Chemical Society and Institute of Materia Medica, Chinese Academy of Medical Sciences.

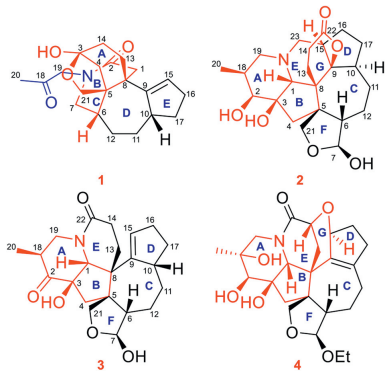


Fig. 1. Chemical structures of compounds **1**–**4**.

as well as their biogenetic precursor (caldaphnidine C). Compound **1** possesses a unique 13-oxa-17-aza-pentacyclo[7.6.4.1^{12,15}.0^{4,8}.0^{9,15}] eicosane core, with the linkage between C-3 and C-14 and the disruption of the C-2–C-18 bond being unprecedented in previously reported DAs. Compounds **2**–**4** have a rearranged 6/5 bicyclic (rings A and B), while **2** also possesses a novel $C_{23}N$ skeleton generated through the ring formation of C-23/C-15 as well as eleven continuous stereogenic centers. Remarkably, compound **2** markedly enhanced the survival of H9c2 cardiomyocytes under oxygen glucose deprivation and reoxygenation (OGD/R) conditions. Preliminary mechanistic study revealed that **2** displayed cardioprotective activity through affecting the kelch-like ECH-associated protein 1-nuclear factor erythroid 2-related factor 2/heme oxygenase-1 (Keap1-Nrf2/HO-1) antioxidant pathway, which could provide a candidate molecule for the further development of treatments for AMI. Herein, the structure elucidation, proposed biosynthetic pathway, and bioactivity evaluation of compounds **1**–**4** are presented.

The molecular formula of compound **1**, $C_{21}H_{29}NO_4$, was established from high resolution electrospray ionization mass spectroscopy (HRESIMS) (*m/z* 360.2175 $[M+H]^+$, calcd. 360.2169), corresponding to eight indices of hydrogen deficiency (IHD). The ^{1}H nuclear magnetic resonance (NMR) spectrum showed one methyl group [δ_H 2.09 (3H, s)] and one olefinic proton (δ_H 5.82). Combined with its distortionless enhancement by polarization transfer (DEPT), heteronuclear single quantum correlation (HSQC), and heteronuclear multiple-bond correlation (HMBC) spectra, the ^{13}C NMR data of **1** (Table S1 in Supporting information) revealed 21 carbon signals, including two carbonyls (δ_C 174.5 and 204.4), two olefinic carbons (δ_C 153.0 and 130.0). Apart from the aforementioned four carbons, the remaining seventeen carbon signals were assigned to three non-protonated carbons (one hemiacetal carbon at δ_C 106.1), two methines, eleven methylenes (one oxygenated carbon at δ_C 76.2, two nitrogen-bearing carbons at δ_C 60.5 and 54.3), and one methyl carbon (δ_C 27.4). Considering the presence of two carbonyl groups and one olefinic group, the occurrence of five unassigned IHD indicated that compound **1** possessed a pentacyclic framework.

Compound **1** was determined to feature an unprecedented 13-oxa-17-aza-pentacyclo[7.6.4.1^{12,15}.0^{4,8}.0^{9,15}] eicosane core by detailed analysis of its 2D NMR spectrum. Two independent spin coupling systems could be deduced from the ^{1}H–^{1}H correlation spectroscopy (COSY) spectrum of **1** (Fig. 2). The HMBC correlations from H_2–1 to C-2, C-5, C-8 and C-9; from H_2–7 to C-2 and C-5; from H-6 and H_2–12 to C-5; from H-15 to C-8 and C-10, coupled with the comparison of chemical shifts of the congeners with similar fragment [19–21], sufficiently facilitated the construction of a 7/7/5 (rings C–E) tricyclic systems. Furthermore, the HMBC correlations from H_2–13 to C-3, C-5, and C-8; from H_2–14 to C-3, C-4, and C-8; and from H_2–4 to C-3, C-5, C-8, and C-14 revealed the presence of cyclohexane structure (ring A). In addition, a 2-oxopropyl

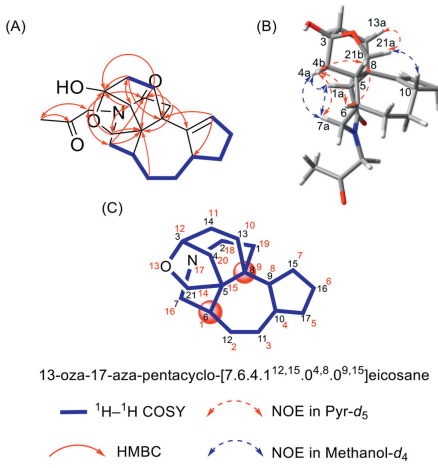


Fig. 2. (A) Key ^{1}H–^{1}H COSY and HMBC correlations of compound **1**. (B) Key NOESY correlations of compound **1**. (C) The nomenclature of the unusual bridged pentacyclic system (numbering in red) of compound **1**.

side chain was inferred to be attached to the nitrogen atom based on the chemical shift of C-19 (δ_C 60.5) and the HMBC correlations from H_3–20 to C-18 and C-19 together with from H_2–19 to C-2 and C-7. Lastly, the HMBC correlations from H_2–21 to C-3, C-4, C-5, and C-6, combined with the remaining one IHD and the chemical shifts of C-3 (δ_C 106.1) and C-21 (δ_C 76.2) disclosed the presence of a furan ring (ring B). The planar structure of compound **1** was thereby established.

The relative configuration of compound **1** was assigned through analysis of the nuclear Overhauser effect spectroscopy (NOESY) spectrum (Fig. 2), where H_2–21 at δ_H 4.40 and 3.97 correlated with H_2–13a and H-6, respectively, confirming the relative configurations of C-5, C-6, and C-8, with H-6 designated as β-oriented. Due to overlapping signals between H-10 and H_2–4a at δ_H 2.84 and between H_2–1a and H_2–19b at δ_H 3.66 in pyridine-d_5, we employed methanol-d_4 as the solvent for NMR testing of compound **1**, which provided distinct signals for these protons (Table S1). The NOESY correlation of H_2–21a and H-10 confirmed that H-10 was also β-oriented. Additionally, the presence of a methylene bridge between C-3 and C-5 rendered the 6-oxabicyclo[3.2.1] octane (rings A and B) in compound **1** a rigid structure, naturally fixing the orientation of the C-3–C-4 bond in the α-direction. The inference was supported by the NOESY correlations of H_2–4a /H_2–1a and H_2–7a, as well as H_2–4b /H_2–7a and H-6. Finally, the absolute configurations of compound **1** were established using electronic circular dichroism (ECD) calculation. As illustrated in Fig. S1 (Supporting information), the calculated ECD curves for compound **1** closely aligned with the experimental one, allowing for the assignment of its absolute configuration, as depicted in Fig. 1.

The HRESIMS data of compound **2** revealed a molecular formula of $C_{23}H_{33}NO_6$, corresponding to eight IHD. The ^{13}C NMR spectrum resolved 23 carbon resonances corresponding to five quaternary carbons (two oxygenated carbons at δ_C 101.8 and 79.7, and one carbonyl carbon at δ_C 173.6), seven methines (one oxygenated carbon at δ_C 73.3, one nitrogen-bearing carbon at δ_C 84.0, and one hemiacetal carbon at δ_C 104.9), ten methylenes (one oxygenated carbon at δ_C 75.2, two nitrogen-bearing carbons at δ_C 59.9 and 54.3), and one methyl, which were distinguished with the aid of HSQC and DEPT experiments. The above-mentioned information suggested compound **2** to be a heptacyclic alkaloid.

The ^{1}H–^{1}H COSY spectrum revealed the presence of three spin systems in compound **2** (Fig. S2 in Supporting information). In the HMBC spectrum, the correlations from H-1 to C-2, C-3, C-4, C-8, C-9, C-19, and C-23; from H_2–4 to C-1, C-2, C-3, C-5, C-6, and C-8; from H-6 to C-5 and C-8; from H-10 to C-9 and C-15; and from H_2–

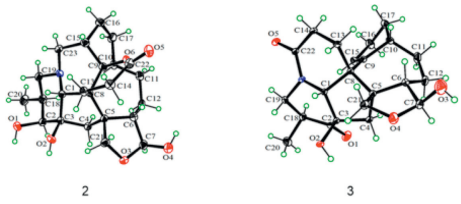


Fig. 3. X ray structure of compounds **2** and **3**.

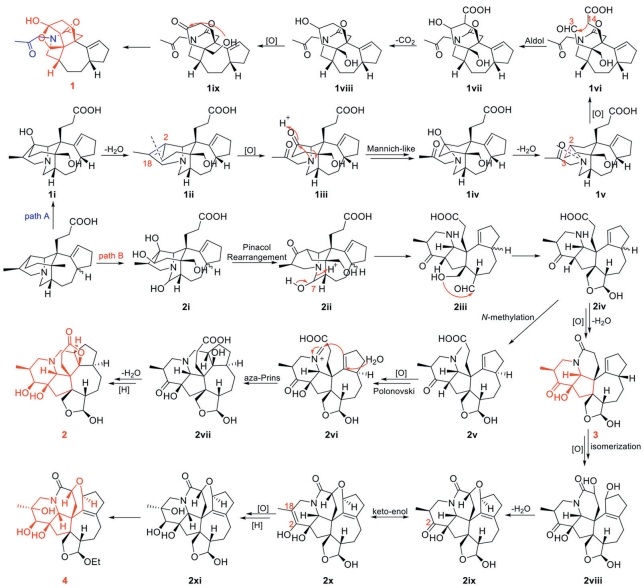
23 to C-9 and C-19 led to the establishment of a partial structure of rings A–E. Furthermore, the HMBC correlations from H_2–21 to C-5, C-6, C-7, and C-8, coupled with the chemical shifts of C-7 (δ_C 104.9) and C-21 (δ_C 75.2) supported the presence of a furan ring (ring F). Lastly, the HMBC correlations from H_2–13 to C-8, C-9, and C-22, along with the remaining one IHD and the chemical shifts of C-9 (δ_C 101.8) and C-22 (δ_C 173.6) revealed the existence of a δ-lactone (ring G). Hence, compound **2** was successfully constructed as a novel 6/5/7/5/6/5/6 seven-ring skeleton.

The network of NOESY correlations including H_2–13/H_2–21b, H-1, and H-15, H_2–21b/H-6, H_2–19b/H-1 and H_3–20 revealed that these protons were on the same side of the molecular plane and were arbitrarily assigned in β-orientation. Therefore, the NOESY correlations of H_2–4a/H-2 and H-10, as well as H_2–4b/H-7 showed that they were α-oriented. The relative configuration of OH-3 could not be accurately determined due to insufficient NOESY signals. Fortunately, after numerous attempts, crystals of compound **2** suitable for X-ray diffraction experiments were successfully obtained from an optimized binary solvent system ($MeOH/CH_2Cl_2/H_2O$, 9:1:0.1). The X-ray structure (Fig. 3) not only confirmed the planar structure inferred from the NMR data but also definitively established its relative configuration. As shown in Fig. S1, the ECD calculation of (1*R*, 2*S*, 3*R*, 5*R*, 6*S*, 7*S*, 8*R*, 9*R*, 10*S*, 15*S*, 18*S*)-**2** was consistent with the experimental result, which assigned its absolute configuration.

The molecular formula of $C_{22}H_{29}NO_5$ for compound **3** was determined by the NMR data and (+)-HRESIMS ion at *m*/*z* 388.2123 $[M+H]^+$ (calcd. 388.2118), indicative of nine IHD. The 1D NMR data of **3** (Table S2 in Supporting information) closely resembled that of the known compound daphnimacropodine A [21], with the primary difference being that the 5/6 bicyclic system (rings A and B) in daphnimacropodine A was substituted with a 6/5 bicyclic system (rings A and B) in **3**. The HMBC correlations from H-1 to C-2, C-3, C-4, C-8, and C-19; from H_2–4 to C-2, C-3, C-5, and C-8; and from H_3–20 to C-2, along with the ^1H–^1H COSY correlations of H_3–20/H-18/H_2–19 enabled the establishment of the rearranged rings A and B. The partial relative configuration of compound **3** was elucidated by its NOESY data (Fig. S3 in Supporting information). The single crystal was successfully obtained from methanol solvent at room temperature, enabling the single-crystal X-ray diffraction analysis (Cu Kα) to confirm the planar structure and the absolute configuration as depicted in Fig. 1, with a Flack's parameter of 0.07(7).

The structure of compound **4** was established by the comprehensive spectroscopic data analyses. Detailed structural elucidation was described in the Supporting information.

A plausible biosynthetic pathway for compounds **1**–**4** was proposed in Scheme 1. Initially, compound **5** (caldaphnidine C) could be converted to **1**iii through a series of hydroxylation, dehydration, and oxidation reactions. Following this, **1**iv was formed through an Mannich-like reaction and simultaneous proton migration [13,22]. Next, the C-2–C-3 bond broke through further dehydration and oxidation reactions. The cyclohexane (ring A) structure was produced through subsequent transformation steps, including aldol and decarboxylation reactions [23–26]. Finally, through oxidation and intramolecular hemiacetal reactions [21], compound **1** was generated



Scheme 1. Plausible biosynthetic pathway of compounds **1**–**4**.

(path A). Compounds **2**–**4** were proposed to be derived from compound **5** and its C-10 isomer (path B). Starting from the hydroxylation at positions C-2, C-3, C-7, and C-21 [21], the key intermediate **2**i could be yielded. The rearranged rings A and B were then formed through a pinacol rearrangement reaction [27]. Subsequently, cleavage of the C-7–N bond and intramolecular hemiacetal reaction could lead to the generation of **2**iv [21]. From this critical intermediate **2**iv, two distinct pathways diverge: on the one hand, intermediate **2**iv underwent a cascade of *N*-methylation, oxidation, and Polonovski reactions to generate **2**vi [24,25], which underwent aza-Prins, esterification, and reduction reactions to form compound **2** [28,29]. On the other hand, intermediate **2**iv underwent formation of the C-22–N bond and oxidation reactions to generate compound **3**. Following this, compound **3** was subjected to double bond isomerization [33], oxidation, and dehydration reactions to yield **2**ix. Ultimately, through keto-enol tautomerization [34,35], oxidation, reduction, and ethylation reactions, compound **4** was generated.

We evaluated the protective effects of the isolated compounds on H9c2 cardiomyocytes under OGD/R conditions. We first assessed cell viability using the CCK-8 assay, and the results showed that compound **2** significantly enhanced cell survival (Fig. 4A). Further dose-dependent experiments revealed that the protective effect of compound **2** increased with concentration, demonstrating a clear dose-response relationship (Fig. 4B), suggesting its potential as a cardioprotective agent. To further investigate whether compound **2** could inhibit OGD/R-induced reactive oxygen species (ROS) production, we measured intracellular ROS levels using flow cytometry and the fluorescent probe DCFH-DA. The results indicated that compound **2** significantly reduced ROS generation in H9c2 cells following OGD/R treatment (Figs. 4C and D), indicating its ability to mitigate oxidative stress and protect cardiomyocytes from hypoxic injury. Additionally, we examined the impact of compound **2** on apoptosis using flow cytometry. The data showed that compound **2** markedly decreased the proportion of early and late apoptotic cells (Figs. 4E and F), demonstrating its capacity to inhibit apoptosis and further supporting its protective role. To elucidate the molecular mechanisms underlying the protective effects of compound **2**, we performed Western blot analysis, focusing on key proteins in the Keap1/Nrf2/HO-1 signaling pathway. The results revealed that compound **2** dose-dependently inhibited Keap1 pro-

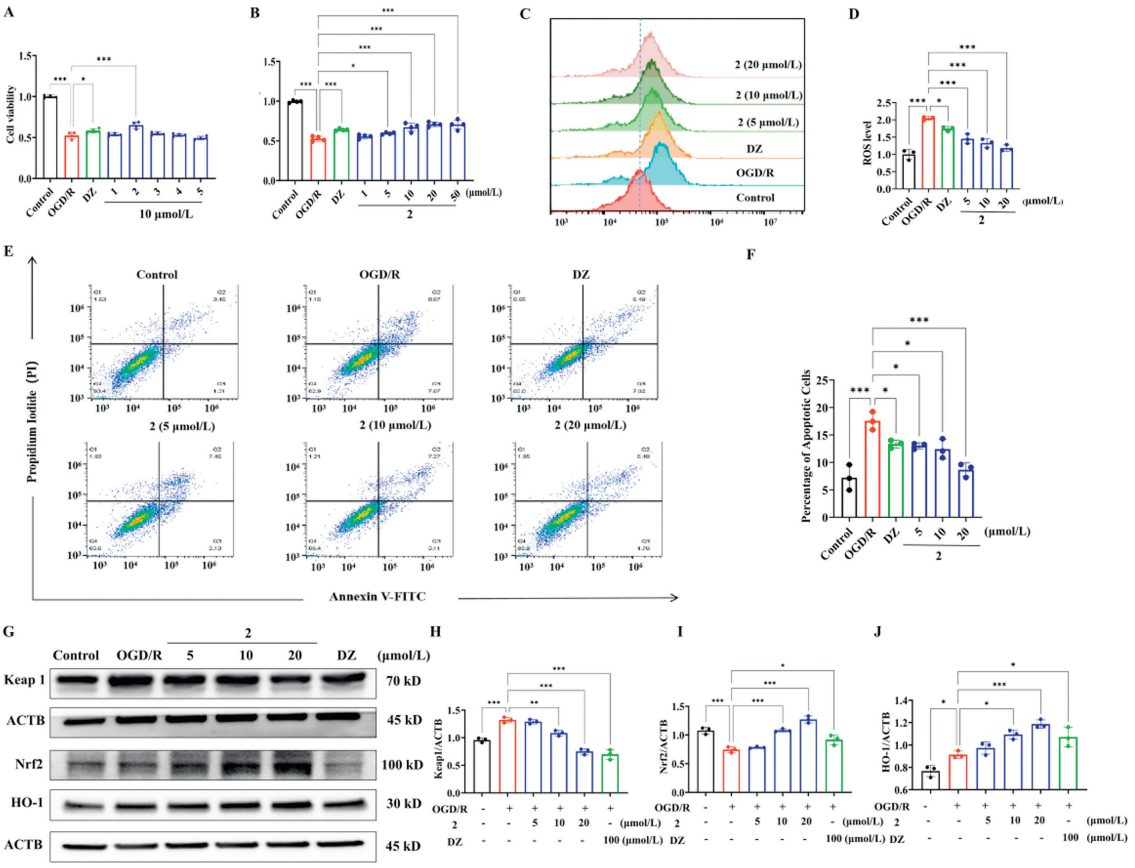


Fig. 4. Protective effects of compound **2** on OGD/R-induced injury in H9c2 cardiomyocytes. (A) The cell viability changes of compounds **1**–**5** under OGD/R conditions in H9c2 cells are illustrated ($n = 4$). (B) Dose-dependent experiments demonstrate the protective effects of compound **2** at various concentrations ($n = 4$). (C, D) Flow cytometry and the fluorescent probe DCFH-DA were used to measure the impact of compound **2** on intracellular ROS generation in H9c2 cells ($n = 3$). (E, F) Flow cytometry was employed to evaluate the effect of compound **2** on the proportion of early and late apoptotic cells in H9c2 cells following OGD/R treatment ($n = 3$). (G–J) Protein expression levels of Keap1, Nrf2, and HO-1 in H9c2 cells after intervention with compound **2** under OGD/R conditions ($n = 3$). DZ: diazoxide, 100 μmol/L. $^{*}P < 0.05$, $^{**}P < 0.01$, $^{***}P < 0.001$. The data are presented as the mean ± SEM and were analyzed using one-way ANOVA followed by the Tukey-Kramer *post hoc* test.

tein expression, stabilized Nrf2 protein levels, and promoted HO-1 expression (Figs. 4G–J). These findings suggested that compound **2** exerted its protective effects by activating the Nrf2/HO-1 antioxidant pathway, thereby enhancing cellular antioxidant capacity and alleviating oxidative stress induced by hypoxia.

In conclusion, we have described four novel alkaloids from *D. calycinum* with intricate and diverse polycyclic skeletons, substantially enriching the structural diversity of DAs. The biosynthetic pathways for the four unusual alkaloids have been also proposed. Additionally, we initially discovered that DAs possessed the potential for cardioprotective activity, and related mechanism studies have been conducted. The discovery of daphcalycines A–D (**1**–**4**) not only enriches the diversity of DAs skeletons but also opens up new perspectives for development on DAs as cardioprotective agents.

Declaration of competing interest

The authors declare that they have no known competing financial interest or personal relationships that could have appeared to influence the work reported in this paper.

CRediT authorship contribution statement

Ji-Hui Zhang: Methodology, Investigation, Data curation, Conceptualization. **Hui-Lin Ou:** Resources. **Ting Lu:** Software. **Si-Yu Yang:** Validation. **Ding Luo:** Validation. **Peng Wu:** Visualization. **Yao-Lan Li:** Resources, Project administration. **Neng-Hua Chen:** Methodology, Investigation. **Guo-Cai Wang:** Writing – review & editing, Writing – original draft, Funding acquisition. **Yu-Bo Zhang:** Writing – review & editing, Writing – original draft, Visualization.

Acknowledgments

This work was supported by the National Natural Science Foundation of China (Nos. 82273803 and 82173695), the Guangdong Basic and Applied Basic Research Foundation (Nos. 2023A1515011896 and 2020A1515110453), Guangzhou Basic and Applied Basic Research (Nos. SL2024A04J0113 and 202102080022), Fundamental Research Funds for the Central Universities (No. 21623224), and the high-performance public computing service platform of Jinan University. The authors gratefully acknowledge the assistance of Huanyong Li, Lin Wang, and Wen Li from the Analytical and Testing Center of Jinan University for the single crystal characterizations, NMR, and HRMS analysis, respectively.

Supplementary materials

Supplementary material associated with this article can be found, in the online version, at doi:10.1016/j.cclet.2025.111314.

References

[1] O. Chehab, A.S. Qannus, M. Eldirani, et al., Cardiol. Res. 9 (2018) 293–299.
[2] Y.Y. Cheng, Z.Y. Xia, Y.F. Han, et al., Oxidative Med. Cell. Longev. 2016 (2016) 2060874.

[3] M.L. Ding, Y.W. Bao, H. Liang, et al., Front. Pharmacol. 15 (2024) 1368765.
[4] D.J. Newman, G.M. Cragg, J. Nat. Prod. 83 (2020) 770–803.
[5] A.K. Chattopadhyay, S. Hanessian, Chem. Rev. 117 (2017) 4104–4146.
[6] L.L. Xu, Z.P. Niu, D.Z. Chen, et al., Phytochemistry 223 (2024) 114106.
[7] Q. Tang, X.Y. Dai, Q. Lin, et al., Chin. J. Chem. 42 (2024) 35–42.
[8] J.B. Xu, H. Zhang, L.S. Gan, et al., J. Am. Chem. Soc. 136 (2014) 7631–7633.
[9] J. Yang, X. Liu, J. Fu, et al., RSC Adv. 11 (2021) 9057–9066.
[10] W.H. Zhang, M. Lu, L. Ren, et al., J. Am. Chem. Soc. 145 (2023) 26569–26579.
[11] L.D. Guo, Y. Zhang, J.P. Hu, et al., Nat. Commun. 11 (2020) 3538–3543.
[12] B.Y. Wang, B. Xu, W. Xun, et al., Angew. Chem. Int. Ed. 60 (2021) 9439–9443.
[13] D.D. Zhang, J.B. Xu, Y.Y. Fan, et al., J. Org. Chem. 85 (2020) 3742–3747.
[14] J.P. Hu, J. Xu, Chin. Chem. Lett. 35 (2024) 108733.
[15] P. Chen, L.J. Liang, Y.F. Zhu, et al., Chin. Chem. Lett. 35 (2024) 109229.
[16] H.J. Wang, Q.Y. Dong, Q.X. Xie, et al., Chin. Chem. Lett. 31 (2020) 685–688.
[17] C.R. Zhang, H.B. Liu, S.H. Dong, et al., Org. Lett. 11 (2009) 4692–4695.
[18] Z.J. Zhan, C.R. Zhang, J.M. Yue, Tetrahedron 61 (2005) 11038–11045.
[19] C.S. Li, Y.T. Di, H.P. He, et al., Org. Lett. 9 (2007) 2509–2512.
[20] H. Morita, H. Takatsu, Y.C. Shen, et al., Tetrahedron Lett. 45 (2004) 901–904.
[21] N.C. Kong, H.P. He, Y.H. Wang, et al., J. Nat. Prod. 70 (2007) 1348–1351.
[22] B.B. Gao, W.Y. Li, S. Jiang, et al., Org. Chem. Front. 11 (2024) 1163–1168.
[23] P.R. Cao, M. Li, J.S. Zhang, et al., Org. Lett. 24 (2022) 6789–6793.
[24] X.X. Zhu, Y.Y. Fan, L. Xu, et al., Org. Lett. 21 (2019) 1471–1474.
[25] D. Xia, Z.H. Wang, J.M. Jiang, et al., Org. Lett. 24 (2022) 4684–4688.
[26] Z.X. Hu, Y. Wu, S.S. Xie, et al., Org. Lett. 19 (2017) 258–261.
[27] Y.T. Di, H.P. He, H.Y. Liu, et al., Tetrahedron Lett. 47 (2006) 5329–5331.
[28] C.Q. Fan, S. Yin, J.J. Xue, et al., Tetrahedron 63 (2007) 115–119.
[29] R.B. Ruggeri, M.M. Hansen, C.H. Heathcock, et al., J. Am. Chem. Soc. 110 (1988) 8734–8736.
[30] J.H. Zhang, J.H. Wang, W. Tang, et al., Chin. J. Nat. Med. 23 (2025) 377–384.
[31] Z.N. Wu, N.H. Chen, Q. Tang, et al., Org. Lett. 22 (2020) 7310–7314.
[32] D. Luo, X.Y. Dai, H. Tian, et al., Phytomedicine 116 (2023) 154909.
[33] C.Y. Zhang, Y.L. Li, Z.J. Chu, et al., Chin. Chem. Lett. 35 (2024) 108206.
[34] J.Y. Zhang, F. Liu, Q. Jin, et al., Chin. Chem. Lett. 35 (2024) 108881.
[35] Q. Li, M. Zhang, X.T. Zhang, et al., Chin. Chem. Lett. 35 (2024) 108193.